HHS Public Access

Author manuscript

Cell Stem Cell. Author manuscript; available in PMC 2017 July 07.

Published in final edited form as:

Cell Stem Cell. 2016 July 7; 19(1): 23–37. doi:10.1016/j.stem.2016.06.001.

Leukemic stem cells evade chemotherapy by metabolic adaptation to an adipose tissue niche

Haobin Ye[1,3], **Biniam Adane**[1], **Nabilah Khan**[1], **Timothy Sullivan**[2], **Mohammad Minhajuddin**[1], **Maura Gasparetto**[1], **Brett Stevens**[1], **Shanshan Pei**[1], **Marlene Balys**[4], **John M. Ashton**[4], **Dwight J. Klemm**[2], **Carolien M. Woolthuis**[6], **Alec W. Stranahan**[6], **Christopher Y. Park**[6], and **Craig T. Jordan**[1,*]

[1]Division of Hematology, University of Colorado, Aurora, CO, 80045

[2]Cardiovascular Pulmonary Research Lab, University of Colorado, Aurora, CO, 80045

[3]Department of Pathology, University of Rochester Medical Center, Rochester, NY, 14642

[4]Functional Genomics Center, University of Rochester Medical Center, Rochester, NY 14642

[6]Human Oncology and Pathogenesis Program, Memorial Sloan Kettering Cancer Center, New York, NY 10065

SUMMARY

Adipose tissue (AT) has previously been identified as an extra-medullary reservoir for normal hematopoietic stem cells (HSCs) and may promote tumor development. Here, we show a subpopulation of leukemic stem cells (LSCs) can utilize gonadal adipose tissue (GAT) as a niche to support their metabolism and evade chemotherapy. In a mouse model of blast crisis CML, adipose-resident LSCs exhibit a pro-inflammatory phenotype and induce lipolysis in GAT. GAT lipolysis fuels fatty acid oxidation in LSCs, especially within a subpopulation expressing the fatty acid transporter CD36. CD36+ LSCs have unique metabolic properties, are strikingly enriched in AT, and are protected from chemotherapy by the GAT microenvironment. CD36 also marks a fraction of human blast crisis CML and AML cells with similar biological properties. These findings suggest striking interplay between leukemic cells and adipose tissue to create a unique microenvironment that supports the metabolic demands and survival of a distinct LSC subpopulation.

*Corresponding author: Craig T. Jordan, University of Colorado Denver, Anschutz Medical Campus, 12700 E 19th Ave, Aurora, CO 80045, craig.jordan@ucdenver.edu.

The authors declare no competing financial interests.

AUTHOR CONTRIBUTIONS

H.Y. and C.T.J designed the experiments and wrote the paper. H.Y. performed all the experiments with the help from B.A., N.K., T.S., M.M., B.S., M.B., J.M.A, S.P., M.G., and C.M.W.. J.M.A. and D.J.K provided technical support. C.Y.P. provided CD36KO mice. H.Y. analyzed data.

INTRODUCTION

Clinical studies have shown that survival for obese leukemia patients is poor relative to normal weight patients (Gelelete et al., 2011; Meloni et al., 2001), suggesting that leukemia cells residing in adipose tissue may be more resistant to treatment and therefore contribute to disease persistence/relapse. Further, numerous studies have demonstrated the unique biology of the adipose tissue microenvironment (Blogowski et al., 2012). However, the nature of interactions between leukemia cells and adipose tissue (AT) is poorly understood and was therefore, the focus of studies described herein.

AT is multifunctional. It serves as a storage site for lipids and also functions as an endocrine organ (Rosen and Spiegelman, 2014). Besides its canonical role in the regulation of systemic metabolism, AT is thought to play a role in the development and progression of solid tumors through various mechanisms (Khandekar et al., 2011). For example, in obese patients, AT contributes to the chronic inflammatory state that induces DNA damage and leads to colon carcinogenesis by production of pro-inflammatory cytokines (adipokines) (Kiraly et al., 2015; Meira et al., 2008). Further, AT has been reported to facilitate the metastasis of ovarian cancer through regulating cancer cell fatty acid metabolism as well as to promote the progression of breast cancer through modulating tumor microenvironment stromal components (Iyengar et al., 2005; Nieman et al., 2011). While these studies suggest a supportive role of AT in multiple steps of carcinogenesis, the biological behaviors of AT are, in turn, altered by cancer cells. For instance, cancer cell-derived cytokines cause lipolysis of AT, leading to tissue atrophy, which is a hallmark of cancer cachexia syndrome (Das et al., 2011; Petruzzelli et al., 2014). Together, these findings imply an interplay between solid tumors and AT. Whether there is a similar relationship between AT and leukemia cells is not yet clear.

A recently identified function of AT is its role as a reservoir for stem cells including HSCs (Han et al., 2010), suggesting the presence of a distinct HSC niche. Interestingly, stromal components in AT are similar to those in the bone marrow (BM), which are essential regulators of HSC homeostasis (Blogowski et al., 2012). Further, AT secretes multiple cytokines such as CXCL12 to recruit and maintain the function of HSCs (Kim et al., 2014). Leukemia stem cells (LSCs) co-opt the HSC marrow environment to gain survival benefits through hijacking the mechanisms utilized by HSCs to maintain homeostasis. For instance, disruption of interactions between LSCs and their stromal components such as the extracellular matrix (ECM) is an effective means to eradicate LSCs (Jin et al., 2006). Further, studies have shown that leukemia cells are protected from oxidative stress by stromal cells in the microenvironment via regulation of cysteine metabolism (Zhang et al., 2012b). These studies led us to hypothesize that the AT HSC niche may be co-opted by LSCs to support their unique metabolic needs.

Stem cells have unique metabolic characteristics, which are accommodated by the microenvironment (Ito and Suda, 2014). For example, a hypoxic microenvironment is required for HSCs to utilize glycolysis as their main energy pathway and disruption of either the hypoxic niche or glycolysis in HSCs results in impaired stem cell functions (Mantel et al., 2015; Takubo et al., 2013). Further, HSCs show an increased reliance on fatty acid

metabolism. Inhibition of fatty acid oxidation (FAO) in HSCs leads to attenuation of stem cell capability (Ito et al., 2012; Takubo et al., 2013). The degree to which LSC biology is influenced by the microenvironment remains largely unknown. Interestingly, AT is capable of regulating metabolism of resident cells through several mechanisms to promote the survival and growth of cancer cells. For example, AT protects acute lymphoid leukemia (ALL) cells from L-Asparaginase by regulating glutamine metabolism (Ehsanipour et al., 2013). Additionally, AT produces several metabolism-regulating adipokines such as leptin and adiponectin whose receptors are commonly expressed by malignant cells to modulate cancer cell metabolism (Vansaun, 2013). These findings suggest a metabolic regulatory role of AT and prompted us to examine a potential effect of AT on LSC metabolism.

In the present study, we show that gonadal adipose tissue (GAT) serves as a reservoir for LSCs. We find that the interplay between resident leukemia cells and GAT results in lipolysis, which in turn fuels the fatty acid metabolism of leukemia cells. Further, we observe a distinct LSC subpopulation expressing the fatty acid transporter CD36. The CD36+ cells demonstrate a relatively high level of FAO, have a quiescent and drug resistant profile, and are protected by GAT from chemotherapy. Additionally, we find CD36 enhances leukemic colonization of GAT and also contributes to chemo-resistance of LSCs.

RESULTS

Adipose tissue functions as a reservoir for LSCs

A murine model of blast crisis chronic myeloid leukemia (bcCML) was used in this study to investigate the interplay between leukemia cells and AT. The system employs co-expression of the BCR-ABL and Nup98-HOXA9 translocations, each independently monitored using green fluorescent protein (GFP) and yellow fluorescent protein (YFP) expression respectively (Figures S1A and S1B). These translocations are detected in human blast crisis CML and the model has previously been described in detail for studies of leukemia genetics and stem cell biology (Ashton et al., 2012; Dash et al., 2002; Mayotte et al., 2002; Neering et al., 2007).

To investigate the presence of leukemia cells in adipose tissue, animals were established using the bcCML model. At advanced stages of disease, cells were isolated from both gonadal adipose tissue (GAT) and inguinal adipose tissue (IAT). GAT represents the largest visceral fat depot in mice, and IAT is the most prevalent reservoir of subcutaneous fat. In addition, several hematopoietic tissues were isolated for comparison, including bone marrow (BM), spleen, and peripheral blood (PB). Interestingly, the data show that leukemia cells are readily evident in GAT, but only present at very low levels in IAT (Figure 1A). These data suggest that adipose tissue microenvironments may differ substantially with regard to their ability to attract and/or support leukemia cells, a finding supported by previous studies in which biological properties of IAT and GAT have been shown to differ substantially (Tchkonia et al., 2013). To further characterize GAT as a reservoir for leukemia cells, histological analyses were performed (Figure 1B). Leukemia cells are observed in direct contact with adipocytes and are prevalent throughout the adipose tissue.

We next asked whether LSCs were also found in GAT. As reported in previous studies a Sca-1+/Lin− phenotype encompasses all detectable LSCs in the bcCML model (Ashton et al., 2012; Neering et al., 2007). We observed enrichment of phenotypically defined LSCs in GAT relative to the hematopoietic tissues (Figure 1C). To investigate the level of functionally-defined LSCs, the stromal vascular fraction (SVF) was isolated from leukemic GAT, which represents an adipocyte-depleted tissue suspension. Transplantation of SVF into recipient mice showed robust development of leukemia as evidenced by GFP+/YFP+ cells in BM, GAT and spleen (Figure S1C). Limiting-dilution transplantation assays indicate that the frequency of LSCs is slightly higher in GAT-derived leukemia cells compared to BM resident leukemia cells (Figure 1D). Finally, we investigated the composition of leukemic populations that migrate to GAT. Homing assays demonstrated that LSCs are significantly enriched in leukemia cells that localize to GAT (Figure 1E). Taken together, these findings indicate that GAT functions as a reservoir for leukemia cells.

Leukemia cells in GAT are pro-inflammatory

To gain insight into the characteristics of LSCs in adipose tissue, we compared transcriptomes of sorted LSCs from GAT, BM, PB, spleen and their non-leukemic counterparts from BM (NBM) by RNA-seq. The data indicate that LSCs in GAT display a distinct gene expression pattern (Figure 2A) characterized by strong up-regulation of pro-inflammatory cytokines/chemokines (Figure S2A). The most strongly up-regulated pro-inflammatory genes are shown in Figure 2B. The leukemic GAT SVF also shows strong up-regulation of pro-inflammatory genes in comparison to controls (Figure S2B). To ensure that non-leukemic cells were not contributing to the pro-inflammatory phenotype, we also examined expression in the GFP−/YFP− population derived from GAT SVF in leukemic mice (Figure 2C). In comparison to naïve GAT SVF, cytokine/chemokine levels are actually somewhat lower, further indicating that the inflammatory state of GAT is due to resident leukemia cells in SVF (Figure 2C).

One possible physiological consequence of an altered inflammatory state could be increased mobilization of free fatty acid from AT. Notably, we observed severe atrophy of GAT (Figure 2D) as well as loss of body weight (Figure S2C) in leukemic mice. Additionally, despite only a low level of leukemia cells, atrophy of IAT was observed as well (Figure S2D). Further analyses indicated that in contrast to GAT, the non-leukemic population from IAT SVF in leukemic mice is more pro-inflammatory than IAT SVF in normal mice (Figure S2E). Together, these findings indicate cachexia in leukemic mice, where systemic factors lead to weight loss in organs that do not display large leukemia cell burden. Interestingly, we also observed that atrophy of GAT precedes body weight loss during the early stage of leukemia development (Figures S2F and S2G).

To examine whether similar symptoms are observed in other leukemic models, we utilized an MLL-AF9 induced leukemia model in which LSCs have been shown to arise in the granulocyte-macrophage progenitor compartment (GMP) (Krivtsov et al., 2006). This model differs from the bcCML model, where previous studies have shown that the HSC/MPP compartment represents the cell of origin (Neering et al., 2007). Similar to what we found in the blast crisis model, loss of body weight as well as atrophy of GAT was observed in

leukemic mice (Figures S2H and S2I). However, leukemic burden in GAT for the MLL-AF9 model is considerably lower than that in BM (Figure S2J), similar to our findings for IAT in the bcCML model. These findings suggest that localization to GAT may be dependent both on the leukemia cell of origin (i.e. HSC vs. GMP) as well as the specific oncogenes that drive the malignant transformation process.

Leukemic adipose tissue is lipolytic

Next we focused on possible mechanisms controlling atrophy of GAT. Previous studies have indicated that lipolysis is mainly responsible for atrophy of AT in the setting of cancer (Das et al., 2011). To test whether leukemic GAT is lipolytic, we cultured GAT explants from control and leukemic mice and monitored lipolysis rates. As shown in Figure 3A, leukemic GAT releases much more free fatty acid (FFA) than control GAT. In addition, fatty acid binding protein 4 (FABP4), which facilitates the transportation of FFA, is also abundantly secreted by leukemic GAT (Figure 3A). These data were further substantiated by detection of an elevated serum FFA level in leukemic mice (Figure 3B). We also found that leukemic serum is a potent inducer of lipolysis in 3T3-L1 adipocytes as well as in normal GAT explants (Figure S3A). Together, these findings strongly support the conclusion that leukemic GAT is lipolytic.

To determine the molecular basis of lipolysis in leukemic GAT, we examined the expression of lipolysis-related genes. Comparison of control and leukemic GAT showed increased expression of adipose triglyceride lipase (*ATGL*), the gene that encodes the rate-limiting enzyme in lipolysis (Das et al., 2011) (Figures 3C–3D). Further, in leukemic GAT we observed reduced expression of negative regulators of lipolysis - lipoprotein lipase (*LPL*) and cell death activator CIDE-A (*CIDEA)* (Figures 3C–3D). LPL controls the influx of FFA into adipocytes (Ebadi and Mazurak, 2014). CIDEA is a lipid droplet (LD) associated protein that shields LDs from lipases and thus inhibits lipolysis (Nordstrom et al., 2005). These results suggest that leukemic GAT triggers a lipolytic program that induces release of FFA and mobilization of lipids that leads to atrophy of GAT.

To determine if inflammatory factors directly mediate lipolysis, we treated 3T3-L1 adipocytes as well as normal GAT explants with each of the pro-inflammatory cytokines/chemokines elevated in GAT. As shown in Figures 3E and S3B, TNF-a, IL-1α, IL-1β and CSF2 are capable of inducing lipolysis. Furthermore, these four cytokines result in reduced expression of both *LPL* and *CIDEA* in GAT explants and 3T3-L1 adipocytes (Figures 3F and S3C). Additionally, analysis of conditioned medium (CM) from control and leukemic GAT explants as well as serum from control and leukemic mice showed increased secretion of IL-1α, IL-1β, TNF-α and CSF2 (Figures 3G and S3D). These findings suggest that TNF-a, IL-1α, IL-1β and CSF2 secreted by leukemia cells mediates lipolysis.

In addition to the pro-inflammatory cytokines outlined above, we note that fatty acid itself can be a potent pro-inflammatory agent (Snodgrass et al., 2013). Therefore, we hypothesized that FFA from lipolysis would further exacerbate inflammation-induced lipolysis. Indeed, we found that leukemia cells treated with palmitate (PA) have increased expression of *IL-1α* and *IL-1β* while normal BM hematopoietic cells do not (Figure 3H). Conversely, unsaturated fatty acid such as oleic acid (OA) has been reported to have anti-inflammatory effect

(Finucane et al., 2015). We observed that OA represses mRNA expression of pro-inflammatory cytokines in normal cells (Figure S3E); however, this repression is not seen in leukemia cells (Figure S3E). Additionally, one recent study reported the induction of IL-1α by OA through an inflammasome-independent pathway (Freigang et al., 2013). Interestingly, we found that OA but not PA is able to induce IL-1α protein production in leukemia cells (Figure 3I).

Together, these observations indicate that resident leukemia cells contribute to the lipolytic status of GAT by disrupting lipid metabolism in GAT through paracrine signaling of pro-inflammatory cytokines.

Fatty acid oxidation is elevated in LSCs

Next we asked how leukemia cells might benefit from lipolysis of adipose tissue. We hypothesized that increased FFA from lipolysis could serve as an energy source for leukemia cells both in GAT and possibly in other tissues. To investigate this hypothesis, we compared the ability of leukemic vs. non-leukemic cells to utilize fatty acid. As shown in Figure 4A, leukemia cells have a higher fatty acid oxidation (FAO) rate compared to control non-leukemia cells. Furthermore, in examining various cell subpopulations, our data show that LSCs have a higher FAO rate than either more differentiated leukemia cells (lin+ leukemia cells) or their counterparts from normal hematopoietic cells (Figure 4B). Interestingly, treatment of leukemic and normal cells with adipocyte conditioned medium (CM) selectively increases FAO rate in LSCs (Figure 4B). Etomoxir, a CPT1 inhibitor, inhibits FAO in both leukemia cells and normal cells (Figure 4B). Of note, etomoxir only reduces FAO in LSCs by about 60%, suggesting that peroxisomal FAO contributes to a substantial part of the overall FAO in LSCs. In addition, we noticed that LSCs exhibit the highest FAO rate when fatty acid serves as the only energy substrate (Figure S4A).

CD36, a fatty acid transporter, modulates energy metabolism in leukemia cells

To gain insights into the mechanism underlying the high FAO rate in LSCs, we compared the expression of FAO-related genes in LSCs, Lin+ leukemia cells and their non-leukemic counterparts. LSCs show a distinct expression pattern of the FAO-related genes (Figure S4B). Specifically, we found one of the fatty acid transporters, CD36, is highly expressed by LSCs (Figures S4B, S4C and 4C), suggesting that CD36 may contribute to the increased FAO in LSCs. Notably, CD36 is not expressed uniformly in the LSC population, indicating that there may be heterogeneity in the stem cell compartment. To investigate a possible role for CD36 in LSCs, we first asked whether CD36-dependent fatty acid transport was evident in both leukemic and normal hematopoietic cells. To this end, we showed that purified CD36+/Lin− leukemia cells demonstrate a higher fatty acid uptake rate and are preferentially sensitive to the CD36 inhibitor sulfosuccinimidyl oleate (SSO) compared to CD36−/lin− leukemia cells. (Figure S4C). Additionally, using a fluorescent long-chain fatty acid analog, BODIPY-Dodecanoic acid (Liao et al., 2005), we showed that CD36+/lin− normal cells have a higher fatty acid uptake rate and are more sensitive to SSO compared to CD36−/lin− cells (Figure S4E). These results suggest that CD36 functions as a fatty acid transporter in both leukemic and normal hematopoietic cells. Next we asked whether CD36 regulates FAO in LSCs. We found that the FAO rate in total LSCs is selectively reduced by

SSO while FAO rates in Lin+ leukemia cells and their normal counterparts are not (Figure 4D). Subsequent isolation of CD36+ vs. CD36− subpopulations showed that CD36+ LSCs have a much higher FAO rate and are more sensitive to SSO than CD36− LSCs (Figures S4F and 4E).

Taken together, these results indicate that the fatty acid transporter CD36 differentially regulates FAO in LSCs. Furthermore, FAO in different LSC sub-fractions seems to be regulated by different mechanisms.

CD36 expression segregates LSCs into two distinct populations

Since CD36+ LSCs have a high requirement for fatty acid and there is abundant FFA in the GAT microenvironment, we hypothesized that CD36+ LSCs might preferentially localize to GAT. Indeed, we found that CD36+ LSCs are strikingly enriched in GAT (Figure 5A). Further, CD36+ LSCs have a higher tendency to migrate to GAT than to BM (Figure 5B), while homing to BM is comparable between CD36+ and CD36− LSCs (Figure S5A).

The presence of phenotypically primitive CD36+ and CD36− subsets raised the question of whether one or both populations contain true functionally-defined LSCs. To investigate this issue, CD36+ vs. CD36− populations were isolated by flow cytometry and used in transplantation assays. As shown in Figure 5C, both populations were able to recapitulate bulk leukemic disease in secondary recipients. Similarly, when cultured in vitro, these two populations were also able to recreate each other (Figure S5B). Additionally, limiting-dilution transplantation assays indicated a comparable LSC frequency between CD36+ and CD36− populations (Figure 5D). These findings demonstrate that there are at least two phenotypically distinct types of LSCs in the blast crisis model employed for these studies. Notably, phenotypically distinct LSCs have recently been reported within primary human leukemia specimens (Eppert et al., 2011; Sarry et al., 2011).

Next we examined relative metabolic status. As shown in Figure S5C, CD36+ LSCs have a lower ATP content than CD36− LSCs, even though their mitochondrial mass is comparable (Figure S5D). We further examined the response of each population to metabolic stress. CD36+ LSCs are more sensitive to 2-Deoxy-D-glucose (2-DG) and more resistant to the Complex I inhibitor rotenone compared to CD36− LSCs (Figure S5E), suggesting the CD36+ cells are more dependent on glycolysis. These observations indicate that CD36+ and CD36− LSCs are metabolically distinct.

The metabolic properties of CD36+ LSCs - high FAO rate, a low ATP level and sensitivity to inhibition of glycolysis - resemble the metabolic characteristics of quiescent HSCs (Ito et al., 2012; Takubo et al., 2013). Cell cycle analyses showed that CD36+ LSCs are relatively quiescent in comparison to the CD36− subpopulation (Figure 5E). In agreement with this result, CD36+ LSCs have higher expression of cell cycle inhibitors and lower expression of cell cycle promoters (Figure S5F). Interestingly, we do not detect any surface expression of CD36 in normal stem/progenitor populations (Figure S5G), suggesting CD36 is preferentially utilized by a subpopulation of LSCs.

Collectively, these findings indicate that at least two metabolically distinct types of leukemia-initiating cells exist in the blast crisis model, and that energy metabolism can differ as a function of anatomical location and expression of CD36.

CD36+ LSCs are drug resistant and protected from chemotherapy by GAT

Since most conventional chemotherapy agents preferentially target cycling cells, we hypothesized that the more quiescent CD36+ LSCs would be relatively drug resistant. To test this hypothesis, we monitored the viability of CD36+ LSCs, CD36− LSCs and bulk leukemia cells upon ex vivo treatment with different chemotherapeutic drugs including cytarabine (Ara-C), doxorubicin, etoposide, SN-38, and irinotecan (CPT-11), as well as the kinase inhibitor dasatinib. We found that all LSCs, both CD36+ and CD36− were more drug resistance than bulk leukemia cells (Figure S5H). Furthermore, compared to CD36− LSCs, CD36+ LSCs were preferentially drug resistant (Figure S5H). To determine whether drug resistance was also evident in vivo, we treated leukemic mice using a regimen that models the treatment for acute myeloid leukemia (AML) patients (Zuber et al., 2009) and improves survival of leukemic mice (Figure 5F). We found that by the end of chemotherapy, CD36+ LSCs are enriched in BM residual leukemia cells while CD36− LSCs are not (Figure 5G), suggesting that CD36+ LSCs are more drug resistant. Analysis of CD36+ LSCs in GAT also showed strong enrichment after chemotherapy (Figure 5G). Intriguingly, the percentage of CD36+ LSCs in GAT is even higher than BM while the percentage of CD36− LSCs in GAT is reduced (Figure 5G), suggesting preferential survival of CD36+ LSCs in GAT. Together, these findings show that CD36+ LSCs are drug resistant and protected by GAT, implying that the heterogeneity found in LSCs is directly related to drug response in different leukemic sub-populations.

Loss of CD36 decreases leukemic burden in GAT and sensitizes LSCs to chemotherapy

We next investigated whether CD36 plays a role in leukemia migration to GAT. First, we examined LSCs in the MLL-AFP model, where migration to GAT was relatively low. Notably, while CD36 was expressed in some bulk tumor cells, there was no CD36 expression in the LSC populations (Figure S6A). Thus, lack of CD36 correlates with poor infiltration of GAT. To further explore this issue, we established the bcCML model using marrow cells derived from a CD36 knockout (CD36KO) mouse strain (Figure S6B). As shown in Figure 6A, leukemic burden is significantly lower in GAT from animals transplanted with CD36KO leukemia cells compared to leukemia derived from wild type (WT) cells. Importantly, the difference between CD36KO and WT leukemia cells was only evident in GAT, whereas all other tissues examined (BM, spleen and PB) showed no difference as a function of CD36 (Figures 6A and S6C). Additionally, no difference was found in the frequency of phenotypically defined LSC between WT and CD36KO leukemia cells in different tissues (Figures 6B and S6D). Consistent with the decreased leukemic burden in GAT, cachexia symptoms were reduced in KO leukemia mice. We observed less body weight loss (Figure S6E) as well as less atrophy of both GAT and IAT in KO leukemia mice compared to WT leukemia mice (Figures 6C and S6F). Serum FFA level is also lower in KO leukemia mice (Figure 6D). Interestingly, CD36KO leukemia cells produce lower amounts of IL-1α compared to WT leukemia cells in both unstimulated and OA-stimulated conditions (Figure 6E), which potentially explains the reduced cachexia in KO leukemia

mice. Together, these findings indicate that the mobilization of fatty acid from adipose tissue in KO leukemia mice is reduced.

To determine whether the decreased leukemia burden in GAT from KO leukemia mice is due to compromised migration to GAT, we performed homing assays and found that CD36KO LSCs are less localized to GAT compared to WT LSCs (Figure 6F), while there are no differences in the homing ability to BM (Figure S6G).

In terms of metabolic activity, we examined whether fatty acid uptake and FAO are impaired in CD36KO leukemia cells. As shown in Figure S6H, fatty acid uptake is decreased in CD36KO lin− leukemia cells compared to their WT counterparts. Further, FAO rate in CD36KO LSCs is significantly lower and less sensitive to the CD36 inhibitor SSO compared to WT LSCs (Figure 6G).

Lastly, we asked whether loss of CD36 would affect LSC drug sensitivity. We first examined viability of LSCs upon ex vivo treatment. CD36KO LSCs are more sensitive to chemotherapeutic drugs (Figure S6I). To test whether CD36KO LSCs are drug sensitive in vivo, we applied the same chemotherapeutic regimen shown in Figure 5F to WT and KO leukemia mice. We found there are more residual leukemia cells in BM of WT leukemia mice compared to KO leukemia mice after chemotherapy (Figure 6H). Furthermore, LSCs are enriched in BM of WT leukemia mice while similar results are not observed in KO leukemia mice (Figure 6I). Together, our data suggest that CD36 contributes to the survival of LSCs.

CD36 expression segregates primitive human blast crisis CML and AML cells into two functionally distinct populations

Finally, we asked whether our findings in the murine model could be recapitulated in human blast crisis CML cells. To this end, we first examined the expression of CD36 in the CD34+ leukemic compartment which is typically enriched for primitive leukemia cells. Of the 8 primary human specimens available for analysis, 4 had readily detectable CD36+ cells in the CD34+ population (bcCML1, 5, 6 and 8) (Figure 7A). Using the fluorescent fatty acid analog, BODIPY-Dodecanoic acid, we found in all 4 samples the CD36+/CD34+ population had a higher fatty acid uptake rate and were more sensitive to the treatment of SSO relative to CD36−/CD34+ cells (Figures 7B and S7A). These findings suggest that CD36 functions as a fatty acid transporter in human bcCML cells. Of these 4 samples, 3 had sufficient tissue for further analyses (bcCML1, 5 and 6). We examined the FAO rate and found that CD36+/CD34+ cells have a higher FAO rate and are more sensitive to SSO in all 3 samples (Figures 7C and S7B), indicating expression of CD36 is linked to increased FAO, as observed in the mouse model.

To investigate infiltration of GAT, we employed a xenograft model using transplantation of human specimens (bcCML1, 5 and 6) into immune deficient NSG mice. Of the three specimens tested, we observed successful engraftment of bone marrow for two specimens (bcCML1 and bcCML5). The presence of human leukemia cells in GAT was observed for both engrafted specimens (Figures 7D and S7C). Further, we found CD36+/CD34+ cells are enriched in GAT (Figures 7E and S7D). Additionally, CD36+/CD34+ cells show greater

homing to GAT than BM, and the CD36 inhibitor SSO impairs their homing to GAT (Figures 7F and S7E). Notably, we found that serum FFA level is elevated in NSG mice engrafted with bcCML cells (Figure 7G).

To determine whether there is any functional difference between CD36+ and CD36− cells, we examined the cell cycle status of these two populations. Consistent with results from the murine model, CD36+/CD34+ cells are more quiescent compared to CD36−/CD34+ in all three samples (Figure S7F). We further compared their drug sensitivity in vitro and found that CD36+/CD34+ cells are relatively drug resistant in all three samples (Figure S7G). Lastly, we asked whether CD36+/CD34+ cells are also drug resistant in vivo. Animals engrafted with the two specimens were treated with Ara-C for 3 days, followed by analysis of marrow cells by FACS. As shown in Figures 7H and S7H, the CD36+/CD34+ cells from both samples were relatively drug resistant in vivo.

Lastly, to explore whether our findings from human blast crisis CML are evident in other forms of disease, we examined the role of CD36 in eight primary samples derived from acute myelogenous leukemia (AML) patients. To provide a broad analysis, we intentionally chose a range of AML specimen types with varying mutations and cytogenetic abnormalities (Table S1). We first examined the expression of CD36 in the CD34+ leukemic compartment. Similar to bcCML, four of the eight specimens had readily detectable CD36+ cells in the CD34+ population (greater than 1%) (AML5, 6, 7 and 8) (Figure 7I). Further, CD36 functions as a fatty acid transporter in all four samples (Figures 7J and S7I). Of note, other groups have shown that in AML patients, poor prognosis is associated with higher expression of CD36 (Perea et al., 2005), indicating a potential role of CD36 in AML persistence/relapse.

Together, these observations suggest that in at least some human blast crisis CML and AML patients, CD36 also functions as a surface marker to segregate metabolically and functionally distinct primitive populations.

DISCUSSION

Despite intensive research efforts, survival for patients with aggressive forms of myeloid leukemia remains poor. While many studies have focused on leukemia cell intrinsic properties as an important challenge, an increasing number of reports have demonstrated a key role for microenvironmental signals in the biology and drug response of leukemia cells (Konopleva and Jordan, 2011; Zhang et al., 2012a). Because an almost infinite number of potential microenvironments may exist in mammalian organisms, the challenge in defining how various extrinsic factors influence anti-leukemia therapies is formidable. In the present study, we focused on adipose tissue (AT) for two reasons – 1) prognosis for obese patients is worse, and 2) AT has previously been shown to be a reservoir for normal HSCs (Marappagoundar et al., 2010). These observations suggest that LSCs may reside in AT and that the unique microenvironment found in such tissue may protect leukemic cells from drug challenge.

To investigate the role of AT in leukemia pathogenesis, we employed a mouse model of blast crisis CML in which LSCs have previously been described. We also examined primary human leukemia specimens. Collectively, these studies provide evidence supporting several previously unknown aspects of leukemia biology. First, GAT provides a unique microenvironmental niche for primitive leukemia cells. Residence in the adipose niche induces a strongly pro-inflammatory phenotype for leukemic cells, resulting in secretion of cytokines that elevate lipolysis and the release of free fatty acids (FFA). We propose that increased FFA acts to positively reinforce the inflammatory condition of leukemia cells in GAT, and to fuel metabolic processes of leukemic cells in both adipose and hematopoietic tissues, as evidenced by increased fatty acid oxidation for LSCs in both adipose tissue and marrow. Second, we observe that functionally defined LSCs exist in at least two distinct forms, differing in metabolism and cell cycle status. The different types of LSC are characterized by expression of CD36, where expression serves to increase uptake of fatty acids. Intriguingly, CD36+ LSCs preferentially home to GAT, indicating a tropism for a microenvironment in which fatty acids are most readily available. Third, LSCs resident in GAT are preferentially resistant to challenge with conventional chemotherapy drugs, particularly the CD36+ LSCs, which reside in a more quiescent cell cycle state. Taken together, these findings support a model in which leukemic cells co-opt adipose tissue to 1) create a microenvironment that supports systemic growth of leukemic disease and 2) provide a niche that confers a relatively drug-resistant phenotype.

An intriguing line of future investigation will be further analysis to determine the exact molecular details that underlie AT protection of LSCs. We speculate that regulation of resident LSC fatty acid metabolism is one of the mechanisms because 1) our study shows that CD36+ drug resistant LSCs have a higher FAO rate, indicating interplay between FAO and drug resistance; and 2) AT selectively regulates LSC FAO. Additionally, adipokines produced by AT have shown protective effects that could also benefit the survival of resident LSCs (Khandekar et al., 2011). A related question is how fatty acid metabolism confers LSC drug resistance. We propose that regulation of cellular redox status is one possible mechanism. FAO contributes to the cellular NADPH pool (Pike et al., 2011), which is critical for redox balance and survival. High rates of FAO produce large amounts of NADH and acetyl-coA, which in turn can inhibit mitochondrial oxidative activities (Jaswal et al., 2011), and thereby further reduce cellular oxidative stress. Lowered oxidative state favors quiescence as well as “stemness” for leukemia cells, as demonstrated by our previous studies in human AML (Lagadinou et al., 2013). Indeed, the present studies showed a more quiescent state for the CD36+ LSCs (Figure 5E), consistent with their improved resistance to chemotherapy. We also note that enzymes involved in FAO directly interact with anti-apoptotic proteins (Giordano et al., 2005; Paumen et al., 1997), suggesting a potential interplay between FAO and cell survival.

An unexpected finding of our studies was the presence of two metabolically distinct LSC subpopulations, suggesting that metabolic heterogeneity may be an intrinsic property of leukemia biology/pathogenesis. This finding has practical ramifications, since we also observe differential drug response as a function of metabolic state. If these data are corroborated with additional studies in humans, it may be important to incorporate such knowledge into the design of anti-leukemia therapies. In principle, to achieve complete

eradication of the LSC population, it will be necessary to employ therapies that can target metabolically distinct subpopulations. Notably, several studies have suggested an interaction between metabolic and functional heterogeneity. For example, long lived and quiescent cells including HSCs and memory T cells have high FAO rates, and disruption of FAO results in dysfunction of these cells (Cui et al., 2015; Ito et al., 2012; van der Windt et al., 2012). These observations lead us to postulate that selective modulation of LSC metabolism could be one component of regimens designed to more effectively eradicate LSC populations. Indeed, previous studies have shown that inhibition of FAO sensitizes leukemia cells to apoptosis stimulators (Samudio et al., 2010).

In summary, our findings demonstrate that GAT in leukemia mice functions as a reservoir for LSCs and confers chemo-resistance to resident leukemia cells, implying a potential role of GAT in the pathogenesis of leukemia and relative efficacy of therapeutic challenge. Furthermore, our data indicate metabolic heterogeneity within LSC populations, where pathways controlling energy consumption can differ. We propose that metabolic heterogeneity in LSCs may contribute to the challenge in effectively eradicating such cells and that modulation of fatty acid metabolism may be a promising way to eradicate LSCs.

EXPERIMENTAL PROCEDURES

Generation of the blast crisis CML Mouse Model

The mouse model was created as described previously (Ashton et al., 2012; Neering et al., 2007). Briefly, 8- to 10-week-old female naive C57Bl6J mice were purchased from Jackson Laboratories. BM from CD36 knock-out mice (B6.129S1-*Cd36*^{tm1Mfe}/J) were a gift from Dr. Christopher Y. Park's lab. BM cells were harvested and mature lineage-positive cells were depleted using BD IMAG immunoaffinity kit per manufacturer instructions. LSK cells were isolated using fluorescently conjugated antibodies for Sca-1 and c-Kit and BD FACS ARIA II cell sorter. LSK cells were cultured in LSK medium (IMDM containing 10% FBS (Thermo Scientific), 10ng/ml IL-3 and IL-6, 50ng/ml SCF and Flt3L (all recombinant murine cytokines were purchased from Peprotech), 1X antibiotic-antimycotic (Thermo Scientific) and 50μg/ml gentamicin (Thermo Scientific)) and infected with viral supernatant twice a day for 3 days and subsequently injected through the retro-orbital sinus into recipient 8- to 10-week-old naive B6.SJL-*PtprcaPepcb*/BoyJ mice (Jackson Laboratories). BM cells and spleens cells from leukemic mice were harvested and frozen for future usage. All animal experiments were approved by University Committee on Animal Resources (UCAR) at the University of Rochester and the Office of Laboratory Animal Resources (OLAR) at the University of Colorado Denver.

Human blast crisis CML xenograft model and chemotherapy in NSG mice

NOD *scid* gamma mice, NSG, (Jackson Laboratories) were transplanted with human leukemia cells via the retro-orbital sinus (5 million/mouse). Four weeks after transplantation, mice were treated with Ara-C (100mg/kg/day) or saline for 3 days and then the composition of BM residual leukemia cells was examined.

Human primary blast crisis CML and AML cells

Primary blast crisis CML and AML cells were obtained from apheresis product, peripheral blood, or bone marrow of patients who gave informed consent for sample procurement.

Statistical analysis

Biological factors were investigated for their relevance by two-tailed Student's t-test with unpaired analysis. $P<0.05$ was considered significant.

Supplementary Material

Refer to Web version on PubMed Central for supplementary material.

Acknowledgments

This work was supported by the NIH (CTJ, R01CA166265: CYP, R01CA164120). AWS is supported by 5TL1TR000459 and 5T32GM008539. We thank Drs. James DeGregori, Eric Pietras, and Dan Sherbenou for critical review and comments.

References

Ashton JM, Balys M, Neering SJ, Hassane DC, Cowley G, Root DE, Miller PG, Ebert BL, McMurray HR, Land H, et al. Gene sets identified with oncogene cooperativity analysis regulate in vivo growth and survival of leukemia stem cells. Cell stem cell. 2012; 11:359–372. [PubMed: 22863534]

Blogowski W, Ratajczak MZ, Zyzniewska-Banaszak E, Dolegowska B, Starzynska T. Adipose tissue as a potential source of hematopoietic stem/progenitor cells. Obesity (Silver Spring). 2012; 20:923–931. [PubMed: 22282043]

Cui G, Staron MM, Gray SM, Ho PC, Amezquita RA, Wu J, Kaech SM. IL-7-Induced Glycerol Transport and TAG Synthesis Promotes Memory CD8(+) T Cell Longevity. Cell. 2015; 161:750–761. [PubMed: 25957683]

Das SK, Eder S, Schauer S, Diwoky C, Temmel H, Guertl B, Gorkiewicz G, Tamilarasan KP, Kumari P, Trauner M, et al. Adipose triglyceride lipase contributes to cancer-associated cachexia. Science. 2011; 333:233–238. [PubMed: 21680814]

Dash AB, Williams IR, Kutok JL, Tomasson MH, Anastasiadou E, Lindahl K, Li S, Van Etten RA, Borrow J, Housman D, et al. A murine model of CML blast crisis induced by cooperation between BCR/ABL and NUP98/HOXA9. Proceedings of the National Academy of Sciences of the United States of America. 2002; 99:7622–7627. [PubMed: 12032333]

Ebadi M, Mazurak VC. Evidence and mechanisms of fat depletion in cancer. Nutrients. 2014; 6:5280–5297. [PubMed: 25415607]

Ehsanipour EA, Sheng X, Behan JW, Wang X, Butturini A, Avramis VI, Mittelman SD. Adipocytes cause leukemia cell resistance to L-asparaginase via release of glutamine. Cancer research. 2013; 73:2998–3006. [PubMed: 23585457]

Eppert K, Takenaka K, Lechman ER, Waldron L, Nilsson B, van Galen P, Metzeler KH, Poeppl A, Ling V, Beyene J, et al. Stem cell gene expression programs influence clinical outcome in human leukemia. Nature medicine. 2011; 17:1086–1093.

Finucane OM, Lyons CL, Murphy AM, Reynolds CM, Klinger R, Healy NP, Cooke AA, Coll RC, McAllan L, Nilaweera KN, et al. Monounsaturated fatty acid-enriched high-fat diets impede adipose NLRP3 inflammasome-mediated IL-1beta secretion and insulin resistance despite obesity. Diabetes. 2015; 64:2116–2128. [PubMed: 25626736]

Freigang S, Ampenberger F, Weiss A, Kanneganti TD, Iwakura Y, Hersberger M, Kopf M. Fatty acid-induced mitochondrial uncoupling elicits inflammasome-independent IL-1alpha and sterile vascular inflammation in atherosclerosis. Nature immunology. 2013; 14:1045–1053. [PubMed: 23995233]

Gelelete CB, Pereira SH, Azevedo AM, Thiago LS, Mundim M, Land MG, Costa ES. Overweight as a prognostic factor in children with acute lymphoblastic leukemia. Obesity (Silver Spring). 2011; 19:1908–1911. [PubMed: 21720424]

Giordano A, Calvani M, Petillo O, Grippo P, Tuccillo F, Melone MA, Bonelli P, Calarco A, Peluso G. tBid induces alterations of mitochondrial fatty acid oxidation flux by malonyl-CoA-independent inhibition of carnitine palmitoyltransferase-1. Cell death and differentiation. 2005; 12:603–613. [PubMed: 15846373]

Han J, Koh YJ, Moon HR, Ryoo HG, Cho CH, Kim I, Koh GY. Adipose tissue is an extramedullary reservoir for functional hematopoietic stem and progenitor cells. Blood. 2010; 115:957–964. [PubMed: 19897586]

Huang S, Rutkowsky JM, Snodgrass RG, Ono-Moore KD, Schneider DA, Newman JW, Adams SH, Hwang DH. Saturated fatty acids activate TLR-mediated proinflammatory signaling pathways. Journal of lipid research. 2012; 53:2002–2013. [PubMed: 22766885]

Ito K, Carracedo A, Weiss D, Arai F, Ala U, Avigan DE, Schafer ZT, Evans RM, Suda T, Lee CH, et al. A PML-PPAR-delta pathway for fatty acid oxidation regulates hematopoietic stem cell maintenance. Nature medicine. 2012; 18:1350–1358.

Ito K, Suda T. Metabolic requirements for the maintenance of self-renewing stem cells. Nature reviews Molecular cell biology. 2014; 15:243–256. [PubMed: 24651542]

Iyengar P, Espina V, Williams TW, Lin Y, Berry D, Jelicks LA, Lee H, Temple K, Graves R, Pollard J, et al. Adipocyte-derived collagen VI affects early mammary tumor progression in vivo, demonstrating a critical interaction in the tumor/stroma microenvironment. The Journal of clinical investigation. 2005; 115:1163–1176. [PubMed: 15841211]

Jaswal JS, Keung W, Wang W, Ussher JR, Lopaschuk GD. Targeting fatty acid and carbohydrate oxidation--a novel therapeutic intervention in the ischemic and failing heart. Biochimica et biophysica acta. 2011; 1813:1333–1350. [PubMed: 21256164]

Jin L, Hope KJ, Zhai Q, Smadja-Joffe F, Dick JE. Targeting of CD44 eradicates human acute myeloid leukemic stem cells. Nature medicine. 2006; 12:1167–1174.

Khandekar MJ, Cohen P, Spiegelman BM. Molecular mechanisms of cancer development in obesity. Nature reviews Cancer. 2011; 11:886–895.

Kim D, Kim J, Yoon JH, Ghim J, Yea K, Song P, Park S, Lee A, Hong CP, Jang MS, et al. CXCL12 secreted from adipose tissue recruits macrophages and induces insulin resistance in mice. Diabetologia. 2014; 57:1456–1465. [PubMed: 24744121]

Kir S, White JP, Kleiner S, Kazak L, Cohen P, Baracos VE, Spiegelman BM. Tumour-derived PTH-related protein triggers adipose tissue browning and cancer cachexia. Nature. 2014; 513:100–104. [PubMed: 25043053]

Kiraly O, Gong G, Olipitz W, Muthupalani S, Engelward BP. Inflammation-induced cell proliferation potentiates DNA damage-induced mutations in vivo. PLoS genetics. 2015; 11:e1004901. [PubMed: 25647331]

Konopleva MY, Jordan CT. Leukemia stem cells and microenvironment: biology and therapeutic targeting. Journal of clinical oncology: official journal of the American Society of Clinical Oncology. 2011; 29:591–599. [PubMed: 21220598]

Krivtsov AV, Twomey D, Feng Z, Stubbs MC, Wang Y, Faber J, Levine JE, Wang J, Hahn WC, Gilliland DG, et al. Transformation from committed progenitor to leukaemia stem cell initiated by MLL-AF9. Nature. 2006; 442:818–822. [PubMed: 16862118]

Lagadinou ED, Sach A, Callahan K, Rossi RM, Neering SJ, Minhajuddin M, Ashton JM, Pei S, Grose V, O'Dwyer KM, et al. BCL-2 inhibition targets oxidative phosphorylation and selectively eradicates quiescent human leukemia stem cells. Cell stem cell. 2013; 12:329–341. [PubMed: 23333149]

Liao J, Sportsman R, Harris J, Stahl A. Real-time quantification of fatty acid uptake using a novel fluorescence assay. Journal of lipid research. 2005; 46:597–602. [PubMed: 15547301]

Mantel CR, O'Leary HA, Chitteti BR, Huang X, Cooper S, Hangoc G, Brustovetsky N, Srour EF, Lee MR, Messina-Graham S, et al. Enhancing Hematopoietic Stem Cell Transplantation Efficacy by Mitigating Oxygen Shock. Cell. 2015; 161:1553–1565. [PubMed: 26073944]

Marappagoundar D, Somasundaram I, Arachimani A, Sankaran R, Viswanathan P, Kumar S, Vipparala V, Mayakesavan B. Characterization of Human Adipose Tissue Derived Hematopoietic Stem Cell, Mesenchymal Stem Cell and Side Population Cells. International Journal of Biology. 2010; 2:71–78.

Matsunaga T, Takemoto N, Sato T, Takimoto R, Tanaka I, Fujimi A, Akiyama T, Kuroda H, Kawano Y, Kobune M, et al. Interaction between leukemic-cell VLA-4 and stromal fibronectin is a decisive factor for minimal residual disease of acute myelogenous leukemia. Nature medicine. 2003; 9:1158–1165.

Mayotte N, Roy DC, Yao J, Kroon E, Sauvageau G. Oncogenic interaction between BCR-ABL and NUP98-HOXA9 demonstrated by the use of an in vitro purging culture system. Blood. 2002; 100:4177–4184. [PubMed: 12393433]

Meira LB, Bugni JM, Green SL, Lee CW, Pang B, Borenshtein D, Rickman BH, Rogers AB, Moroski-Erkul CA, McFaline JL, et al. DNA damage induced by chronic inflammation contributes to colon carcinogenesis in mice. The Journal of clinical investigation. 2008; 118:2516–2525. [PubMed: 18521188]

Meloni G, Proia A, Capria S, Romano A, Trape G, Trisolini SM, Vignetti M, Mandelli F. Obesity and autologous stem cell transplantation in acute myeloid leukemia. Bone marrow transplantation. 2001; 28:365–367. [PubMed: 11571508]

Neering SJ, Bushnell T, Sozer S, Ashton J, Rossi RM, Wang PY, Bell DR, Heinrich D, Bottaro A, Jordan CT. Leukemia stem cells in a genetically defined murine model of blast-crisis CML. Blood. 2007; 110:2578–2585. [PubMed: 17601986]

Nieman KM, Kenny HA, Penicka CV, Ladanyi A, Buell-Gutbrod R, Zillhardt MR, Romero IL, Carey MS, Mills GB, Hotamisligil GS, et al. Adipocytes promote ovarian cancer metastasis and provide energy for rapid tumor growth. Nature medicine. 2011; 17:1498–1503.

Nordstrom EA, Ryden M, Backlund EC, Dahlman I, Kaaman M, Blomqvist L, Cannon B, Nedergaard J, Arner P. A human-specific role of cell death-inducing DFFA (DNA fragmentation factor-alpha)-like effector A (CIDEA) in adipocyte lipolysis and obesity. Diabetes. 2005; 54:1726–1734. [PubMed: 15919794]

Paumen MB, Ishida Y, Han H, Muramatsu M, Eguchi Y, Tsujimoto Y, Honjo T. Direct interaction of the mitochondrial membrane protein carnitine palmitoyltransferase I with Bcl-2. Biochemical and biophysical research communications. 1997; 231:523–525. [PubMed: 9070836]

Perea G, Domingo A, Villamor N, Palacios C, Junca J, Torres P, Llorente A, Fernandez C, Tormo M, Queipo de Llano MP, et al. Adverse prognostic impact of CD36 and CD2 expression in adult de novo acute myeloid leukemia patients. Leukemia research. 2005; 29:1109–1116. [PubMed: 16095690]

Petruzzelli M, Schweiger M, Schreiber R, Campos-Olivas R, Tsoli M, Allen J, Swarbrick M, Rose-John S, Rincon M, Robertson G, et al. A switch from white to brown fat increases energy expenditure in cancer-associated cachexia. Cell metabolism. 2014; 20:433–447. [PubMed: 25043816]

Pike LS, Smift AL, Croteau NJ, Ferrick DA, Wu M. Inhibition of fatty acid oxidation by etomoxir impairs NADPH production and increases reactive oxygen species resulting in ATP depletion and cell death in human glioblastoma cells. Biochimica et biophysica acta. 2011; 1807:726–734. [PubMed: 21692241]

Rosen ED, Spiegelman BM. What we talk about when we talk about fat. Cell. 2014; 156:20–44. [PubMed: 24439368]

Samudio I, Harmancey R, Fiegl M, Kantarjian H, Konopleva M, Korchin B, Kaluarachchi K, Bornmann W, Duvvuri S, Taegtmeyer H, et al. Pharmacologic inhibition of fatty acid oxidation sensitizes human leukemia cells to apoptosis induction. The Journal of clinical investigation. 2010; 120:142–156. [PubMed: 20038799]

Sarry JE, Murphy K, Perry R, Sanchez PV, Secreto A, Keefer C, Swider CR, Strzelecki AC, Cavelier C, Recher C, et al. Human acute myelogenous leukemia stem cells are rare and heterogeneous when assayed in NOD/SCID/IL2Rgammac-deficient mice. The Journal of clinical investigation. 2011; 121:384–395. [PubMed: 21157036]

Simsek T, Kocabas F, Zheng J, Deberardinis RJ, Mahmoud AI, Olson EN, Schneider JW, Zhang CC, Sadek HA. The distinct metabolic profile of hematopoietic stem cells reflects their location in a hypoxic niche. Cell stem cell. 2010; 7:380–390. [PubMed: 20804973]

Snodgrass RG, Huang S, Choi IW, Rutledge JC, Hwang DH. Inflammasome-mediated secretion of IL-1beta in human monocytes through TLR2 activation; modulation by dietary fatty acids. Journal of immunology. 2013; 191:4337–4347.

Somervaille TC, Cleary ML. Identification and characterization of leukemia stem cells in murine MLL-AF9 acute myeloid leukemia. Cancer cell. 2006; 10:257–268. [PubMed: 17045204]

Sugiyama T, Kohara H, Noda M, Nagasawa T. Maintenance of the hematopoietic stem cell pool by CXCL12-CXCR4 chemokine signaling in bone marrow stromal cell niches. Immunity. 2006; 25:977–988. [PubMed: 17174120]

Takubo K, Goda N, Yamada W, Iriuchishima H, Ikeda E, Kubota Y, Shima H, Johnson RS, Hirao A, Suematsu M, et al. Regulation of the HIF-1alpha level is essential for hematopoietic stem cells. Cell stem cell. 2010; 7:391–402. [PubMed: 20804974]

Takubo K, Nagamatsu G, Kobayashi CI, Nakamura-Ishizu A, Kobayashi H, Ikeda E, Goda N, Rahimi Y, Johnson RS, Soga T, et al. Regulation of glycolysis by Pdk functions as a metabolic checkpoint for cell cycle quiescence in hematopoietic stem cells. Cell stem cell. 2013; 12:49–61. [PubMed: 23290136]

Tchkonia T, Thomou T, Zhu Y, Karagiannides I, Pothoulakis C, Jensen MD, Kirkland JL. Mechanisms and metabolic implications of regional differences among fat depots. Cell metabolism. 2013; 17:644–656. [PubMed: 23583168]

van der Windt GJ, Everts B, Chang CH, Curtis JD, Freitas TC, Amiel E, Pearce EJ, Pearce EL. Mitochondrial respiratory capacity is a critical regulator of CD8+ T cell memory development. Immunity. 2012; 36:68–78. [PubMed: 22206904]

Vansaun MN. Molecular pathways: adiponectin and leptin signaling in cancer. Clinical cancer research: an official journal of the American Association for Cancer Research. 2013; 19:1926–1932. [PubMed: 23355630]

Wajchenberg BL. Subcutaneous and visceral adipose tissue: their relation to the metabolic syndrome. Endocrine reviews. 2000; 21:697–738. [PubMed: 11133069]

Wang YH, Israelsen WJ, Lee D, Yu VW, Jeanson NT, Clish CB, Cantley LC, Vander Heiden MG, Scadden DT. Cell-state-specific metabolic dependency in hematopoiesis and leukemogenesis. Cell. 2014; 158:1309–1323. [PubMed: 25215489]

Wei J, Wunderlich M, Fox C, Alvarez S, Cigudosa JC, Wilhelm JS, Zheng Y, Cancelas JA, Gu Y, Jansen M, et al. Microenvironment determines lineage fate in a human model of MLL-AF9 leukemia. Cancer cell. 2008; 13:483–495. [PubMed: 18538732]

Yu WM, Liu X, Shen J, Jovanovic O, Pohl EE, Gerson SL, Finkel T, Broxmeyer HE, Qu CK. Metabolic regulation by the mitochondrial phosphatase PTPMT1 is required for hematopoietic stem cell differentiation. Cell stem cell. 2013; 12:62–74. [PubMed: 23290137]

Zhang B, Ho YW, Huang Q, Maeda T, Lin A, Lee SU, Hair A, Holyoake TL, Huettner C, Bhatia R. Altered microenvironmental regulation of leukemic and normal stem cells in chronic myelogenous leukemia. Cancer cell. 2012a; 21:577–592. [PubMed: 22516264]

Zhang W, Trachootham D, Liu J, Chen G, Pelicano H, Garcia-Prieto C, Lu W, Burger JA, Croce CM, Plunkett W, et al. Stromal control of cystine metabolism promotes cancer cell survival in chronic lymphocytic leukaemia. Nature cell biology. 2012b; 14:276–286. [PubMed: 22344033]

Zuber J, Radtke I, Pardee TS, Zhao Z, Rappaport AR, Luo W, McCurrach ME, Yang MM, Dolan ME, Kogan SC, et al. Mouse models of human AML accurately predict chemotherapy response. Genes & development. 2009; 23:877–889. [PubMed: 19339691]

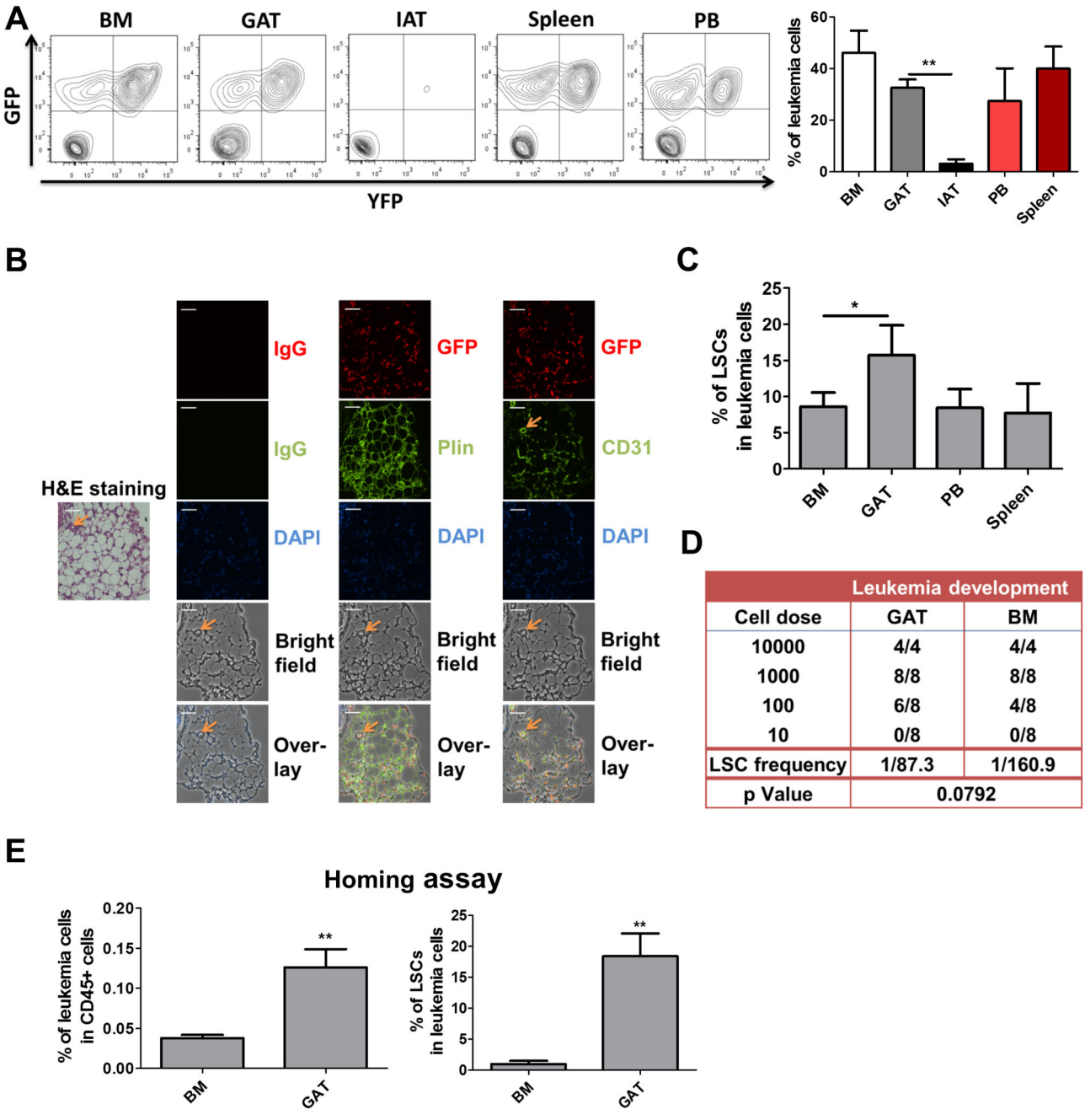

	Leukemia development	
Cell dose	GAT	BM
10000	4/4	4/4
1000	8/8	8/8
100	6/8	4/8
10	0/8	0/8
LSC frequency	1/87.3	1/160.9
p Value	0.0792	

Figure 1. Adipose Tissue Functions as A Reservoir for LSCs

(A) Leukemia cell (GFP+/YFP+) frequency in in multiple tissues (CD45+ cells) – bone marrow (BM), gonadal adipose tissue (GAT), inguinal adipose tissue (IAT), spleen and peripheral blood (PB). Error bars show means ± S. D. n=5, ** P<0.005. (B) Histological analyses of leukemia infiltration of adipose tissue. Hematoxylin and eosin (H&E) labeling of tissue morphology of GAT (20X magnification). Orange arrow indicates a blood vessel identified by CD31 labeling and morphology. Immunofluorescent labeling of GFP (indicated in red) shows extensive infiltration of leukemia cells throughout the adipose tissue. Labeling

with CD31 and Plin indicate endothelial cells and adipocytes respectively. DAPI indicates nuclei of cells. Overlay of all fields (bottom row) shows the position of numerous leukemia cells in direct contact with adipocytes. Scale bar = 50 microns. (C) Frequency of immunophenotypically-defined LSCs in multiple tissues. Error bars show means ± S. D. n=3, * $P<0.05$. (D) Limiting-dilution analysis of LSC frequency in GAT vs. BM. (E) Homing assays to determine the degree of bulk leukemia cell and LSC migration to GAT and BM. Error bars show means ± S. D. n=4, ** $P<0.005$.

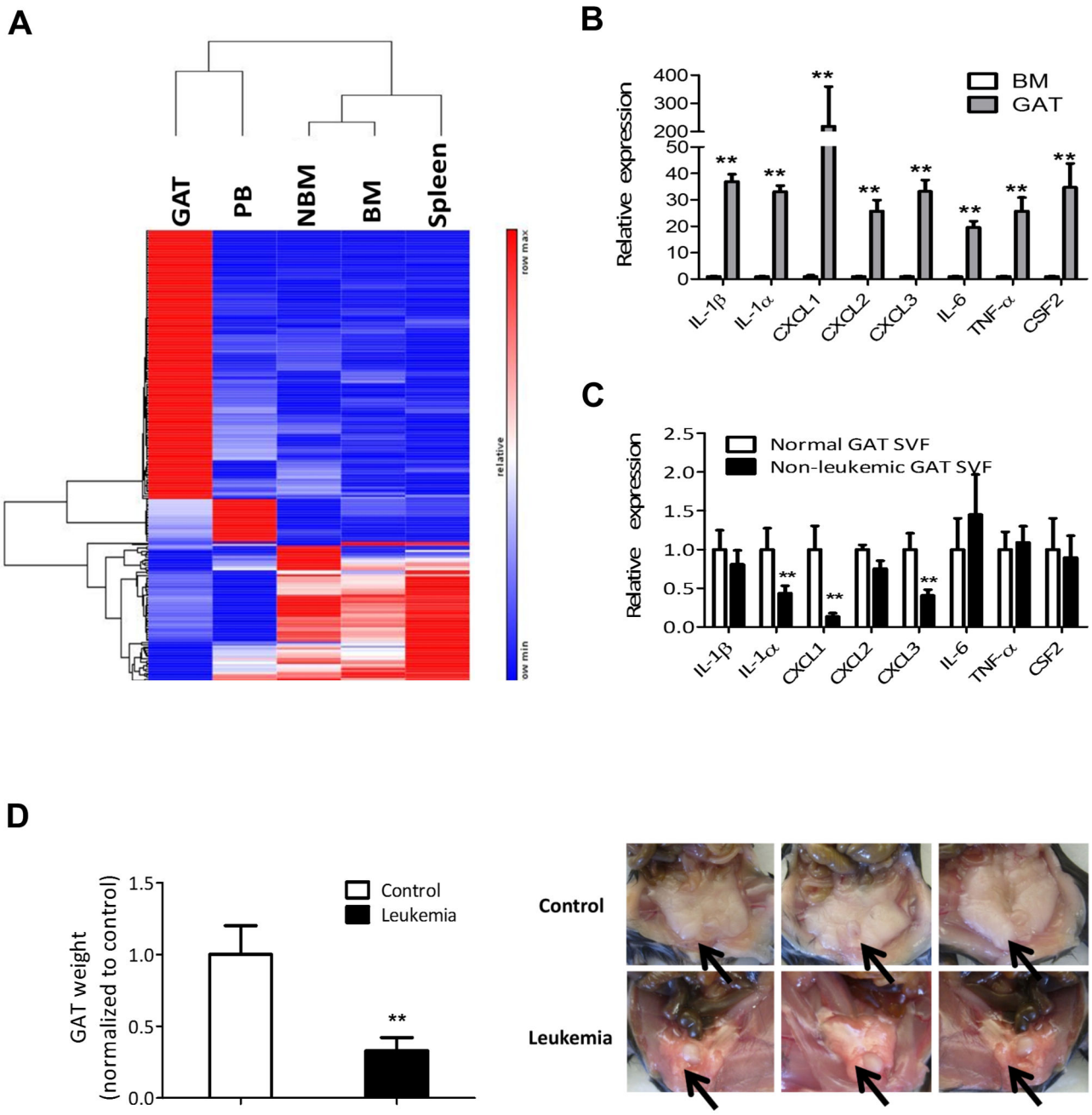

Figure 2. Leukemia Cells in Gonadal Adipose Tissue are Pro-inflammatory

(A) Heat map of genes differentially expressed by LSCs and their non-leukemic BM counterparts (NBM). RNA from LSCs in each tissue and NBM was isolated and subjected to RNA-seq. Three cohorts for each type of LSCs were analyzed. Each cohort consisted of pooled LSCs from ten mice. Genes that are only significantly differentially expressed in all three cohorts were chosen to make the heat map. (Red=up-regulated, Blue=down-regulated). See also Figure S2A. (B) Expression of pro-inflammatory cytokines/chemokines genes in BM leukemia cells and GAT leukemia cells. Error bars show means ± S. D. from triplicates. ** P<0.005. (C) GAT SVF from normal mice and GAT non-leukemic (GFP−/YFP−) SVF

from leukemia mice were isolated by flow cytometric sorting to determine the expression of pro-inflammatory cytokines. Error bars show means ± S. D. from triplicates. ** $P<0.005$. (D) Atrophy of GAT is found in leukemic mice. GAT from control (transplanted with normal BM hematopoietic cells) and leukemic mice was weighted at day 12 after transplantation. Arrows indicate GAT. Error bars show means ± S. D. n=8, ** $P<0.005$.

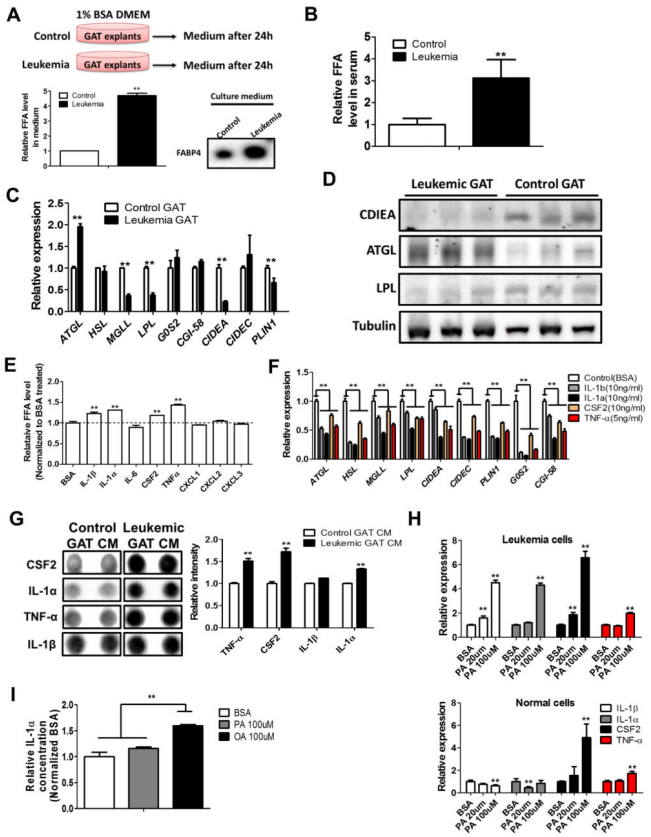

Figure 3. Leukemic Adipose Tissue is Lipolytic

(A) GAT explants (300mg) from control (transplanted with normal BM hematopoietic cells) and leukemic mice were cultured in DMEM containing 1% BSA for 24h and FFA and FABP4 levels in culture medium were determined. Error bars show means ± S. D. from triplicates. ** P<0.005. (B) Serum FFA level in control and leukemic mice. Error bars show means ± S. D. n=8, ** P<0.005. (C) mRNA expression of lipolysis related genes in control and leukemic GAT. Error bars show means ± S. D. from triplicates. ** P<0.005. (D) Protein levels of *ATGL*, *LPL* and *CIDEA* in control and leukemic GAT. Each lane represents GAT from two mice. (E and F) Normal GAT explants were cultured in DMEM containing 1% BSA and indicated cytokines (5ng/ml for TNF-α and 10ng/ml for others) for 24h. FFA level in culture medium (E) and expression of lipolysis related genes (F) were determined. Error bars show means ± S. D. from triplicates. ** P<0.005. (G) Conditioned medium (CM) from control and leukemic GAT was subjected to cytokine arrays. Array results as well as quantification for IL-1α, IL-1β, TNF-α and CSF2 were shown. Error bars show means ± S. D. from the duplicate dots for each cytokines. ** P<0.005. (H) Leukemia and normal BM cells were treated with BSA or palmitate (PA) (20 and 100μm) for 24h and expression of pro-inflammatory cytokines/chemokines genes was determined. Error bars show means ± S. D. from triplicates. ** P<0.005. (I) Leukemia cells (1 million/ml) were treated with BSA, PA (100μm) or oleic acid (OA) (100μm) for 24h, and ELISA was performed to determine the concentration of IL-1α in media. Error bars show means ± S. D. from triplicates. ** P<0.005.

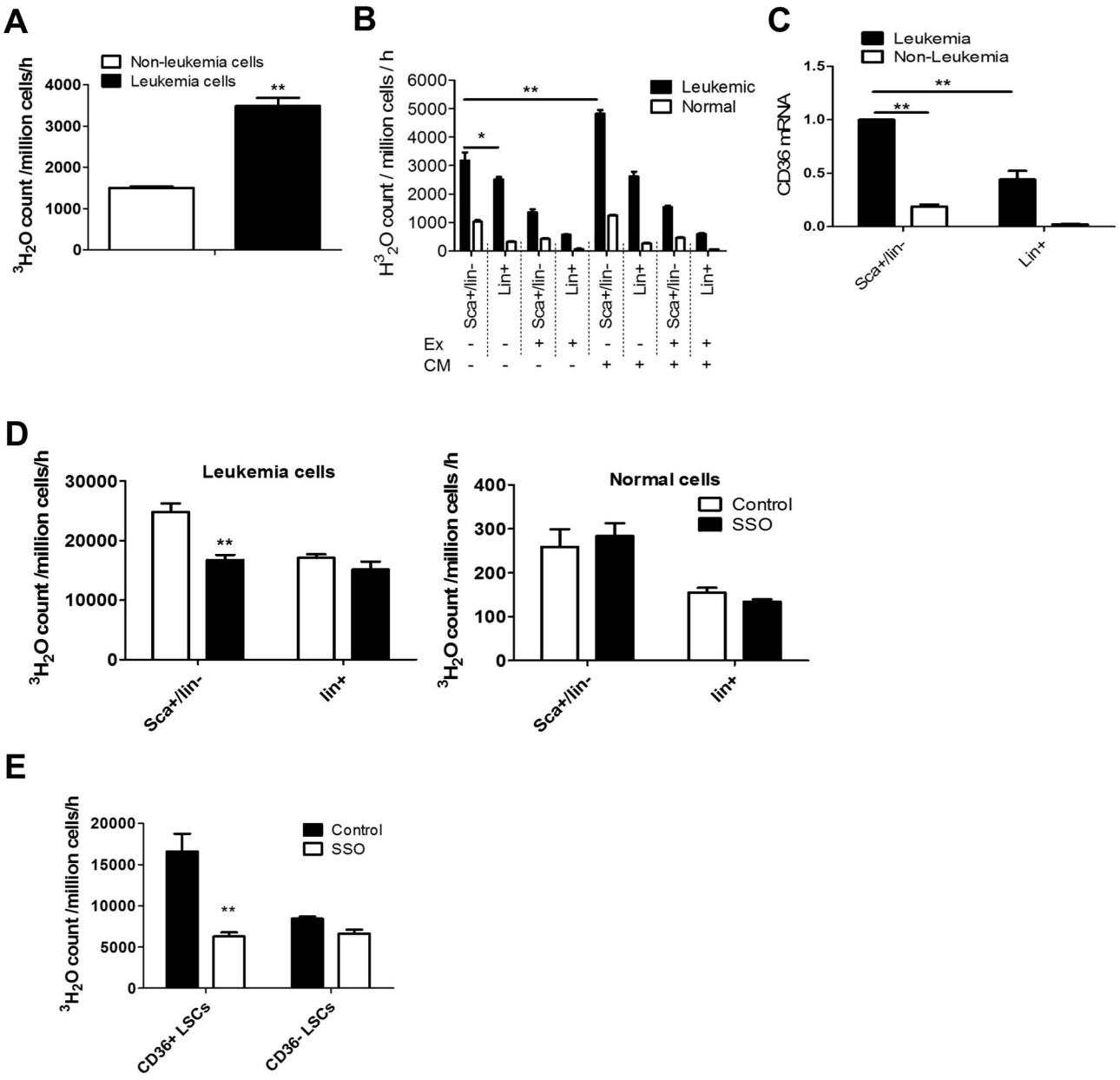

Figure 4. CD36, A Fatty Acid Transporter, Modulates Energy Metabolism in Leukemia Cells

(A) Leukemia cells and non-leukemia cells (GFP−/YFP−) from the same sample were sorted and FAO assays monitoring the release of tritiated water (^3H_2O) from tritium labeled palmitate were performed to determine their FAO rates. Error bars show means ± S. D. from triplicates. ** P<0.005. (B) FAO rates of LSCs, Lin+ leukemia cells and their counterparts from normal BM were determined with or without the presence of adipocytes conditioned medium (CM) or the CPT1 inhibitor etomoxir (Ex) (100uM). Error bars show means ± S. D. from triplicates. * P<0.05, ** P<0.005. (C) Expression of *CD36* mRNA in LSCs, Lin+ leukemia cells and their counterparts. Error bars show means ± S. D. from triplicates. ** P<0.005. (D) FAO rates of LSCs and Lin+ leukemia cells and their counterparts from

normal BM were determined with or without the presence of the CD36 inhibitor SSO (50μM). Error bars show means ± S. D. from triplicates. ** $P<0.005$. (E) FAO rate in CD36+ vs CD36− LSCs in the presence or absence of SSO (50μM). Error bars show means ± S. D. from triplicates. ** $P<0.005$.

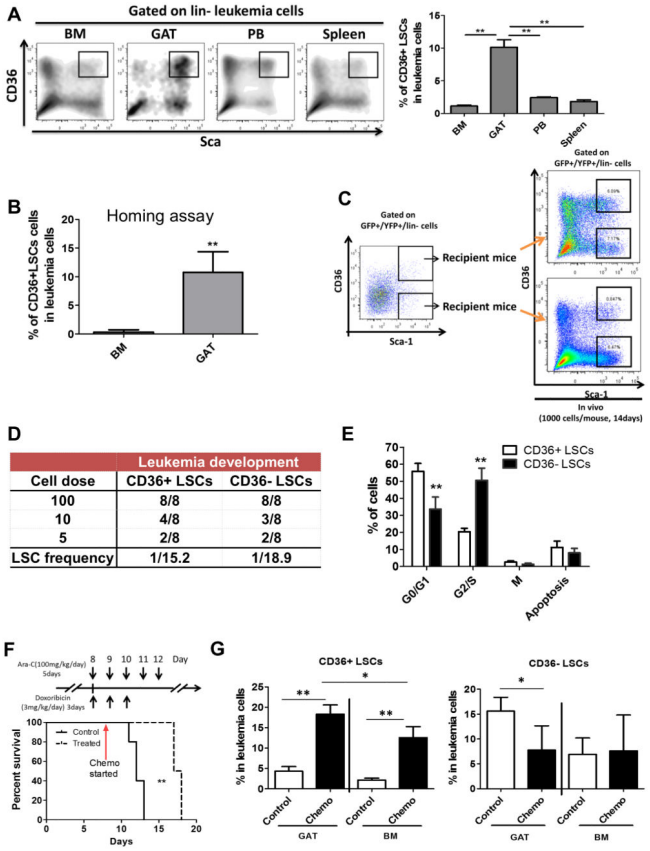

	Leukemia development	
Cell dose	CD36+ LSCs	CD36- LSCs
100	8/8	8/8
10	4/8	3/8
5	2/8	2/8
LSC frequency	1/15.2	1/18.9

Figure 5. CD36 Expression Segregates LSCs into Two Distinct Populations

(A) Frequency of CD36+ LSCs in BM, GAT, PB, and Spleen. Error bars show means ± S. D. n=3, ** P<0.005. (B) Homing ability of CD36+ and CD36− LSCs to GAT. Error bars show means ± S. D. n=3, **P<0.005. (C) Functional analysis of LSC potential in CD36+ vs. CD36− LSCs. Equal numbers of CD36+ and CD36− LSCs were injected into recipient mice (1000 cells/mouse). Two weeks later, BM cells from recipients were collected to examine the composition of leukemia cells. (D) Limiting-dilution analysis of leukemia-initiating cell frequency in CD36+ and CD36− LSCs. (E) Cell cycle status of CD36+ vs CD36− LSCs as determined by in vivo BrdU labeling. Error bars show means ± S. D. n=3, ** P<0.005. (F) Chemotherapy prolongs survival of leukemic mice. Leukemic mice were treated with a chemotherapeutic regimen as described in experimental procedures. Survival of control (vehicle treated) and chemotherapy treated leukemic mice was monitored. n=5, ** P<0.005. (G) Preferential survival of CD36+ LSCs in GAT after chemotherapy. BM and GAT from control (vehicle treated) and chemotherapy treated leukemic mice were harvested and the composition of residual leukemia cells was examined. Error bars show means ± S. D. n=5, * P<0.05, ** P<0.005.

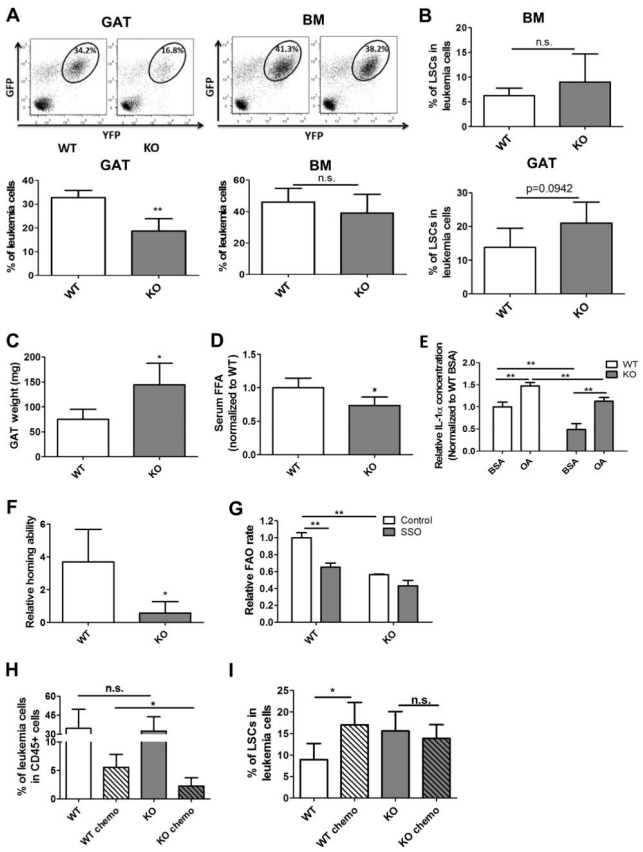

Figure 6. Loss of CD36 decreases leukemic burden in gonadal adipose tissue and sensitizes LSCs to chemotherapy

(A) Leukemia burden in the GAT and BM of wild type (WT) vs CD36 knock-out (KO) leukemia mice. Error bars show means ± S. D. n=5, ** P<0.005. (B) Percentage of LSCs in BM and GAT resident leukemia cells from WT and CD36 KO leukemia mice. Error bars show means ± S. D. n=5. (C) GAT weight in WT and KO leukemia mice. Error bars show means ± S. D. n=5, * P<0.05. (D) Serum FFA level in WT and KO leukemia mice. Error bars show means ± S. D. n=5, * P<0.05. (E) Secretion of IL-1α in WT and CD36KO leukemia cells. Leukemia cells (1 million/ml) were treated with BSA or OA (100μM) for 24h, and ELISA was performed to determine the concentration of IL-1α in media. Error bars show means ± S. D. from triplicates. ** P<0.005. (F) Homing ability of WT and CD36 KO LSCs to GAT. Homing ability of LSCs was determined by the ratio of the percentage of LSCs in the leukemia cells localized to GAT to the percentage of LSCs in leukemia cells before injection. Error bars show means ± S. D. n=4, * P<0.05. (G) FAO rate in WT and CD36KO LSCs. FAO rate was measured with or without the CD36 inhibitor SSO (50 μM). Error bars show means ± S. D. from triplicates. ** P<0.005. (H and I) Percentage of residual leukemia cells (H) as well as LSCs (I) was determined in WT and CD36 KO leukemia mice after chemotherapy. Error bars show means ± S. D. n=5, * P<0.05.

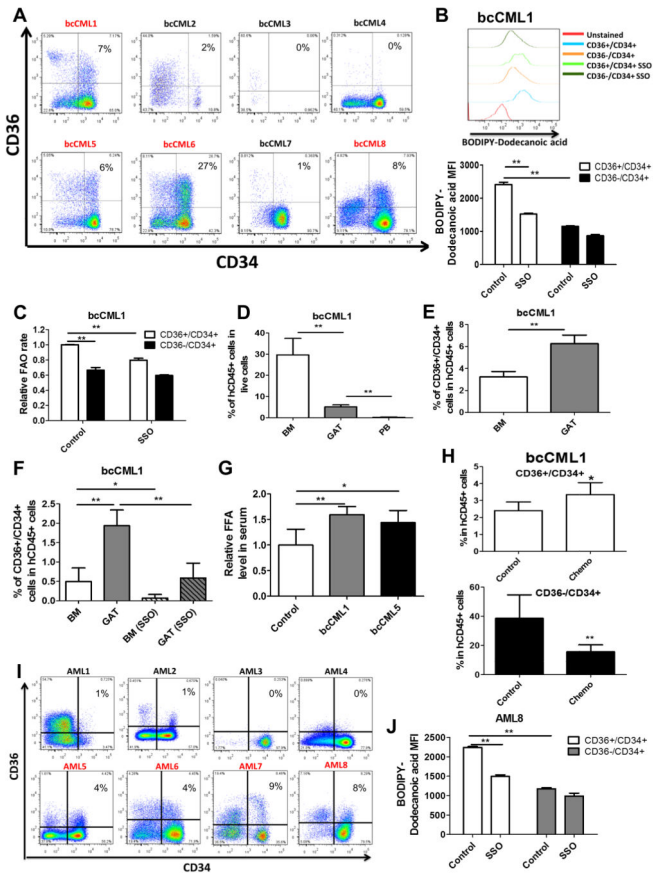

Figure 7. CD36 Expression Segregates Primary Human blast crisis CML and AML cells to Two Functionally Distinct Populations

(A) Expression of CD36 in primary human blast crisis CML (bcCML) cells. Red text indicates specimens with sufficient CD34+/CD36+ cells for subsequent analyses. (B) Fatty acid uptake in bcCML cells. Leukemia cells were serum starved and pre-treated with or without SSO (50μM) before incubation with BODIPY-Dodecanoic acid (1μM). Error bars show means ± S. D. from triplicates. ** P<0.005. See also Figure S7A. (C) FAO rate in CD36+/CD34+ vs. CD36−/CD34+ cells in the presence or absence of CD36 inhibitor SSO (50 μM). Error bars show means ± S. D. from triplicates. ** P<0.005. See also Figure S7B. (D) Leukemia burden in BM, GAT and PB in immune deficient NSG mice transplanted with human bcCML cells. Error bars show means ± S. D. n=5, ** P<0.005. See also Figure S7C. (E) CD36+/CD34+ cells are enriched in GAT relative to BM. Error bars show means ± S. D. n=5, ** P<0.005. See also Figure S7D. (F) Homing ability of CD36+/CD34+ cells to BM and GAT. Leukemia cells were pre-treated with or without SSO (50 μM) for 1h before injection. Error bars show means ± S. D. n=5, ** P<0.005. See also Figure S7E. (G) Serum FFA level in normal NSG mice and NSG mice engrafted with bcCML cells. Error bars show means ± S. D. n=5, * P<0.05, ** P<0.005. (H) NSG mice transplanted with bcCML cells were treated with Ara-C (100mg/kg/day) or saline (control) for 3 days. Composition of BM residual leukemia cells was examined to evaluate relative drug resistance of CD36+/CD34+ vs. CD36−/CD34+ cells. Error bars show means ± S. D. n=4, * p<0.05, ** P<0.005. See also Figure S7H. (I) Expression of CD36 vs CD34 in primary human AML samples. Red

text indicates specimens with sufficient CD34+/CD36+ cells for subsequent analyses. (J) Fatty acid uptake in AML cells. Leukemia cells were serum starved and pre-treated with or without SSO (50μM) before incubation with BODIPY-Dodecanoic acid (1μM). Error bars show means ± S. D. from triplicates. ** $P<0.005$. See also Figure S7I.